VNU Journal of Science: Mathematics - Physics

Journal homepage: https://js.vnu.edu.vn/MaP

Original Article

Numerical Investigation of Dispersion in As_2se_3 Suspended-Core Photonic Crystal Fibers Filled with Carbon Disulfide

Dang Van Trong[1,2], Chu Van Lanh[1], Vo Thi Hong Yen[3], Nguyen Huy Hoang[4], Chu Van Ben[5,*]

[1]*Vinh University, 182 Le Duan, Truong Vinh, Nghe An, Vietnam*

[2] *Nha Trang University, 2 Nguyen Dinh Chieu, Bac Nha Trang, Khanh Hoa, Vietnam*

[3]*Chau Thanh 1 High School, National Route 80, Tan Nhuan Dong Commune, Dong Thap, Vietnam*

[4]*Phan Boi Chau High School for the Gifted, 19 Le Hong Phong, Truong Vinh, Nghe An, Vietnam*

[5]*Posts and Telecommunications Institute of Technology, 96A Tran Phu, Ha Dong, Hanoi, Vietnam*

Received 26th September 2025
Revised 04th November 2025; Accepted 29th December 2025

Abstract: We present a novel study on the dispersion properties of suspended-core fibers fabricated from arsenic selenide glass infiltrated with carbon disulfide. This specific fiber structure, to our knowledge, has not been studied previously. By replacing air holes with carbon disulfide, a significant modification of the dispersion characteristics is achieved, providing flattened and close-to-zero dispersion characteristics in both dispersion regimes. This unique dispersion engineering makes CS_2-infiltrated As_2Se_3 suspended-core fibers highly promising for generating smooth and broadband supercontinuum spectra in the near-infrared region. These results highlight the unexplored potential of this suspended-core fibers for advanced nonlinear photonic applications.

Keywords: Photonic crystal fibers, Suspended-core fibers, Dispersion.

1. Introduction

Based on their geometry, microstructured optical fibers (MOFs) are generally classified into two main categories: hollow-core and solid-core fibers [1-8]. In hollow-core MOFs, the core is typically gas or air (with a low refractive index), while the cladding is made of a high-index material. Light is guided and confined inside the hollow region not by total internal reflection, but primarily through the photonic

* Corresponding author.
E-mail address: bencv@ptit.edu.vn

https//doi.org/10.25073/2588-1124/vnumap.5077

bandgap effect or anti-resonant reflection (depending on the design), enabling efficient power transmission an attractive feature for optical spectroscopy [1]. Nevertheless, a major limitation of hollow-core MOFs is their relatively narrow operational spectral range [2]. Conversely, in solid-core MOFs, light propagation relies on total internal reflection, producing supercontinuum generation (SCG), while only a small fraction of the power couples into the surrounding holes [6-8]. A notable subclass of solid-core MOFs is the suspended-core fiber (SCF), which typically consists of a core with a diameter in the micron or submicron scale held in place by three thin glass bridges [9, 10]. SCFs are also attractive for nonlinear optics application due to the strong confinement of light in the small core [11]. Furthermore, adjusting the core's size and geometry can induce significant birefringence or enhanced nonlinear effects, thereby enabling SC generation with potential applications in areas such as biomedical imaging and chemical sensing [6, 12].

In recent decades, the mid-infrared (mid-IR) region has attracted increasing interest due to its ability to reveal the chemical composition of organic substances through distinct spectral fingerprints [13]. Mid-IR light is particularly important for a variety of applications, including gas detection [6], medical diagnostics [11], and food quality assessment [14]. While fused silica fibers have been widely employed to generate broadband SC in the visible and near-IR regions [6], they suffer from intrinsic transmission limits that restrict their performance in the mid-IR. This limitation motivates the use of alternative nonlinear media beyond silica. To address this challenge, fibers based on non-silica glasses such as tellurite [15], heavy-metal oxide [16], and chalcogenide glasses (ChGs) [17] have been developed for mid-IR SC generation. Additionally, photonic crystal fibers (PCFs) with air holes infiltrated by different liquids have been proposed [18-20]. Liquid infiltration provides a flexible approach to tuning fiber dispersion without altering the structural dimensions, enabling substantial modifications of the dispersion profile.

To meet various application requirements, PCFs are developed with various geometric core structures, such as square, circular, regular hexagonal, octagonal, and suspended cores. In particular, the SCF stands out as an ideal candidate for enhancing improving nonlinear effects and dispersion optimization. Because of its vital contribution to nonlinear optical studies, SCF has been the focus of considerable investigation in recent years. The concept of "suspended-core fiber" was initially proposed by Monro et al., in 2001 [21], followed by works on SCFs made from lead silicate and tellurite glass with high nonlinearity and anomalous dispersion [22, 23]. Next, studies on SCF with sensor applications were introduced [24, 25]. Since then, SCFs have emerged as a distinctive subclass of microstructured fibers.

To improve the SCG generation performance, both theoretical and experimental investigations have examined the influence of the core diameter together with the shape, size, number, and thickness of the glass bridges in SCFs, aiming to enhance birefringence and nonlinear responses. Nevertheless, extending the SC spectrum into the mid-IR range remains difficult when using silica-based PCFs, primarily because of the high phonon energy and intrinsic losses of pure silica [9, 26-28]. As a result, SCFs made from soft glasses have garnered significant attention from scientists due to their high linear refractive index, strong Kerr nonlinearity, mid-to-far infrared optical transparency, exceptional clarity, and enhanced rare-earth solubility [29, 30].

Recently, researchers have explored liquid infiltration in silica-based SCFs, where air holes were filled with liquids such as water [31], $CHCl_3$ [32], and butanol [33]. Similar approaches have also been applied to ChGs-based SCFs ([e.g., PBG-08 [29], NC21A [34], As_2S_3 [35]), particularly with water infiltration, to investigate SCG. Such techniques allow dispersion properties to be modified without altering the geometrical parameters of the fiber, offering greater flexibility in dispersion management. To our knowledge, despite these advances, SCFs made of As_2Se_3 infiltrated with CS_2 have not yet been reported, leaving their potential for dispersion engineering and broadband SCG largely unexplored.

Based on the above analysis, this paper, for the first time, proposes optimizing the dispersion properties of SCFs using As_2Se_3 glass as the substrate material and CS_2-infiltrated air holes. We selected As_2Se_3 as the substrate material to achieve high nonlinearity while mitigating fabrication difficulties. Owing to its relatively low softening temperature (≈180°C), As_2Se_3 enables easier realization of such deformed air-hole structures compared with other highly nonlinear glasses [36, 37]. This study is driven by the interest in CS_2, a commonly available solvent characterized by wide spectral transmission, high nonlinearity, and the absence of significant Raman scattering within its transparent region [38].

The remainder of this paper is arranged as follows. Section 2 introduces the design of the SCF. Section 3 presents and discusses the results, with particular emphasis on the influence of geometrical parameters and the materials infiltrated into the air holes on the fiber characteristics. Finally, Section 4 highlights the principal results and provides the conclusion.

2. Numerical Modeling

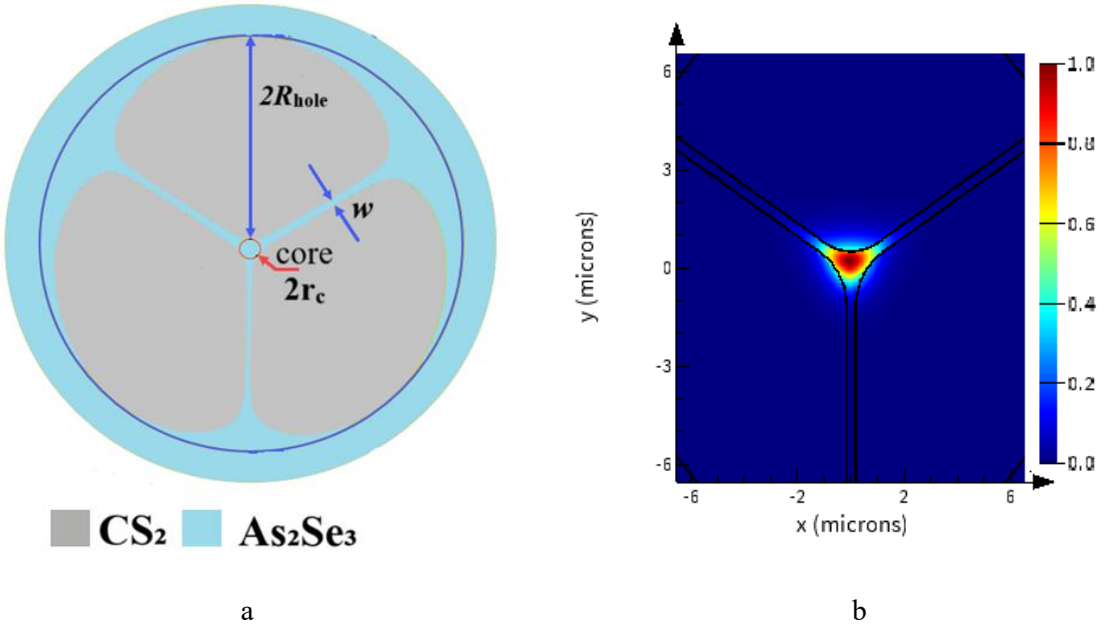

a b

Figure 1. (a) Cross-sectional schematic diagram of CS_2-filled SCF with three bridges (b) The light is confined in the core of CS_2-filled SCF with $w/r_c = 0.8$.

The sensitivity of SCFs to parametric and geometrical modifications allows them to control their optical properties precisely. Such waveguides are characterized by a few basic parameters: R_{hole} (air hole radius), Λ (pitch), r_c (core radius), and w (the width of the bridge) as depicted in Fig. 1. Our SCF, which has three air-hole suspended structures, has cores connected to the glass bridge by circular arc-shaped linkers. The holes are infiltrated by CS_2 with a refractive index $n = 1.628$ in the As_2Se_3 background [38]. If the SCF is designed from the commercially available MODE Solutions software, the finite element method (FEM) is responsible for the mode analysis [39]. It is worth noting that backscattered radiation can give rise to unwanted effects at the simulation boundaries. Therefore, a perfectly matched layer has been added outside the SCF structure to increase the reliability of the obtained results [40]. In this work, we fix the core radius with $r_c = 0.5$ μm, which is within the allowable range of the conventional Stack-

and-draw technology [31]. The ratio between the width of the bridge and the core radius should be optimized to reach the preeminent results for dispersion D. As a result, structures with w/r_c in the range of 0.55−0.95 are studied. The value of Λ in our SCF model is determined by the expression $\Lambda = 2R_{hole} + w$. Air hole radius R_{hole} is determined by formula 1, where N is the number of bridges. Figure 1b shows the field intensity distribution of fundamental modes for the CS_2-filled SCF with $w/r_c = 0.8$. The maximum intensity is observed at the central region of the core.

$$R_{hole} = \left[\frac{w}{2} - r_C \,\mathrm{Sin}\left(\frac{\pi}{N}\right)\right] / \left[\mathrm{Sin}\left(\frac{\pi}{N}\right) - 1\right] \tag{1}$$

The real part of the refractive index n of As_2Se_3 and CS_2 is calculated as a function of wavelength using the Sellmeier formula in Eqs. (2, 3) [41, 42].

$$n_{As_2Se_3} = 1 + \frac{2.234921\lambda^2}{\lambda^2 - 0.24164^2} + \frac{0.347441\lambda^2}{\lambda^2 - 19^2} + \frac{1.308575\lambda^2}{\lambda^2 - 4\times 0.24164^2} \tag{2}$$

$$n_{CS_2} = 1 + \frac{1.50387\times\lambda^2}{\lambda^2 - 0.03049} \tag{3}$$

Fig. 2 shows the real part of refractive index n of As_2Se_3 and CS_2 with wavelength. It can be seen that the refractive index of As_2Se_3 is always greater than that of CS_2. Light transmitted in SCF with an As_2Se_3-core follows the same total internal reflection mechanism as that of conventional optical fibers.

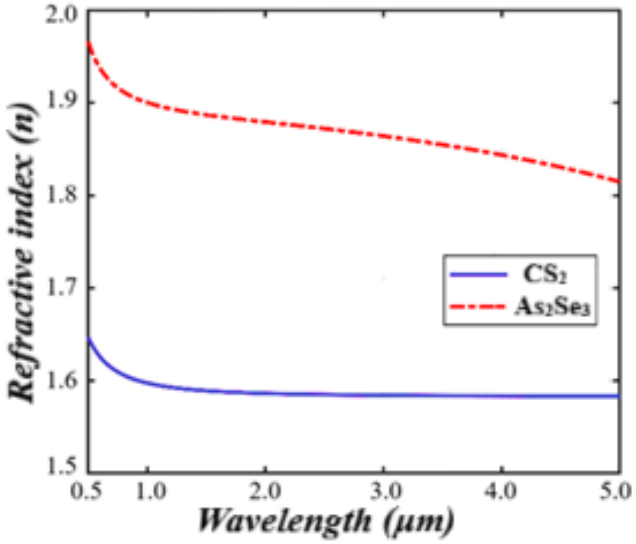

Figure 2. The real part of the refractive index n of As_2Se_3 and CS_2.

The value of chromatic dispersion D for SCFs can be calculated from the wavelength derivative of the real part of the effective refractive index $Re[n_{eff}]$, and is expressed by the following relation, with c representing the velocity of light in vacuum [43]

$$D = -\frac{\lambda}{c}\frac{\partial^2 \mathrm{Re}[n_{\mathrm{eff}}]}{\partial\lambda^2} \tag{4}$$

Table 1. Structural parameters of the investigated fibers

w/r_c	w	N	R_{hole}	Λ
0.55	0.275	3	2.21	4.69
0.6	0.3	3	2.11	4.52
0.65	0.325	3	2.02	4.36
0.7	0.35	3	1.93	4.20
0.75	0.375	3	1.83	4.04
0.8	0.4	3	1.74	3.88
0.85	0.425	3	1.65	3.72
0.90	0.45	3	1.55	3.55
0.95	0.475	3	1.46	3.395

3. Results and Discussion

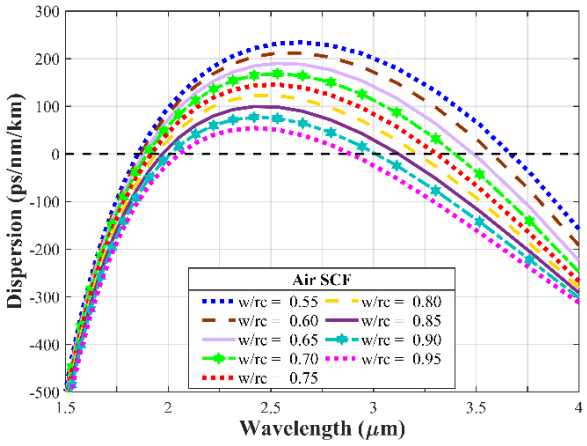

(a)

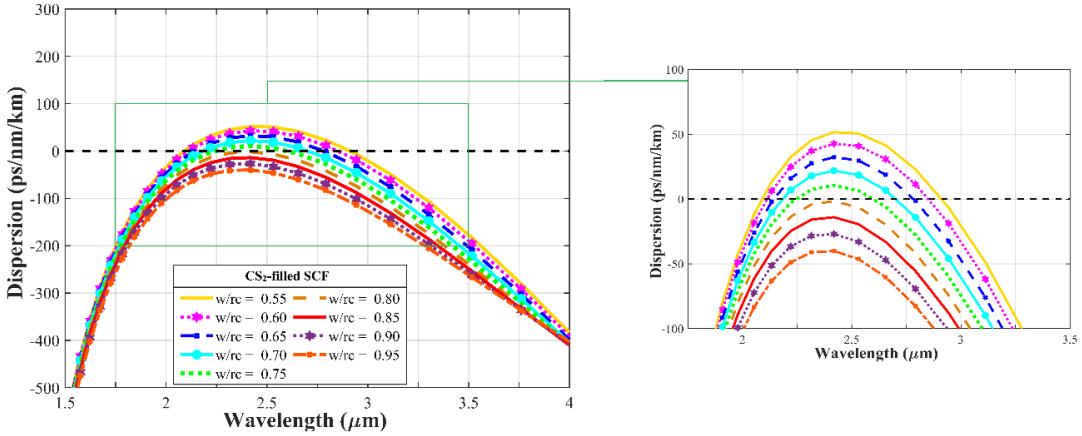

(b)

Figure 3. The dispersion properties of **(a)** unfilled SCF and **(b)** CS_2-filled SCF.

To evaluate the capability of tailoring dispersion in SCFs, we carried out simulations considering different ratios between the bridge width and the core radius (w/r_c). In particular, the dispersion of the fundamental mode was analyzed for two cases: an SCF with air holes and a CS_2-infiltrated SCF, both sharing identical structural parameters (Fig. 3). For clarity, we define the near-zero dispersion (NZD) region as the spectral range where the dispersion remains between -100 and 100 ps/nm/km. Such dispersion profiles are highly favorable for efficient supercontinuum generation.

Considering the scalability of spinning technology, it can be assumed that the overall diameter and related parameters can be adjusted within a feasible range. Hence, in order to provide a more comprehensive analysis, our simulations were performed using several rescaled parameter sets relative to those employed in fiber fabrication. The proposed parameter values are summarized in Table 1.

Fig. 3a shows the effect of varying w/r_c on the dispersion in the case of the SCF infiltrated with air. Looking at the figure, the SCF infiltrated with air has varying dispersion at different wavelengths, and all fibers have an anomalous dispersion regime. The resulting dispersion curves include anomalous dispersion with two zero-wavelength dispersions (ZWDs). In this survey, we observed representative SCF characteristics featuring relatively high anomalous dispersion and ZDWs exceeding 1750 nm.

In the next step, we performed a dispersion study for the SCF infiltrated with CS_2 case with the same structural parameters. Fig. 3b illustrates the dispersion profile of the SCF filled with CS_2. We can see that the dispersion characteristics of the CS_2-filled SCF have a clear change compared to the previous air-infiltrated SCF. The all-normal dispersion configuration usually appears at the structures $w/r_c = 0.8$ and $w/r_c = 0.85$, which the air-infiltrated SCF does not achieve.

Our findings indicate that the w/r_c ratio of the SCF governs the shift of the dispersion curve relative to the dispersion axis and defines the locations of the first and second ZDW. Table 2 shows the ZWDs values for the studied SCFs. The position of ZDW_1 is shifted toward the long wavelength as w/r_c increases. The position of the second ZDWs is shifted toward the short wavelength if w/r_c increases for both cases of the studied SCFs. The change of w/r_c leads to further change of dispersion characteristics. As the w/r_c ratio rises, dispersion flattens, the ZDW is displaced, and all curves shift closer to the normal dispersion region.

Table 2. The values of ZDW of the SCF with various values of w/r_c

w/r_c	Unfilled SCF		CS_2-filled SCF	
	ZDW_1 (μm)	ZDW_2 (μm)	ZDW_1 (μm)	ZDW_2 (μm)
0.55	1.854	3.667	2.091	2.91
0.6	1.867	3.577	2.113	2.849
0.65	1.882	3.485	2.143	2.783
0.7	1.897	3.395	2.185	2.7
0.75	1.918	3.307	2.247	2.596
0.8	1.944	3.213	-	-
0.85	1.973	3.121	-	-
0.90	2.011	3.01	-	-
0.95	2.055	2.887	-	-

We observed that when the air holes of SCF are infiltrated with CS_2, the dispersion characteristics are flatter and the small dispersion value lies in the near-zero dispersion range. This is very good for the generation of high-performance supercontinuum.

When targeting efficient broadband SCG, the air-filled SCFs considered in this study are not viable, as their dispersion profiles do not coincide with the NZD band. The infiltration of CS_2 into the air holes leads to a pronounced modification of the dispersion behavior in SCFs. Compared with air-filled SCF,

CS_2 infiltration consistently produces flatter dispersion profiles. Such behavior has also been widely reported in all-solid PCF [30]. This is a result of reducing the contrast in the fiber structure and introducing materials with non-zero material dispersion instead of air.

All CS_2-filled SCF have flat dispersion characteristics. In particular, the dispersions of the fibers with $w/r_c = 0.7$, $w/rc = 0.75$, $w/rc = 0.8$, and $w/rc = 0.85$ are consistent with the NZD band. The $w/r_c = 0.7$ and $w/r_c = 0.75$ fibers have anomalous dispersion profiles. Therefore, these fibers are good candidates for generating a broad supercontinuum spectrum. Meanwhile, the $w/r_c = 0.8$ and $w/r_c = 0.85$ fibers have a completely normal dispersion profile in all the infrared bands considered. These two fibers are both good candidates for generating a soliton-driven supercontinuum.

A PCF with low and flat dispersion is essential for SCG, as it governs the quality of the output pulses. Therefore, we proposed two optimal fibers for SCG in this study, which are CS_2-infiltrated SCF with parameters $w/r_c = 0.75$ and $w/r_c = 0.8$, respectively, shown in Fig. 4.

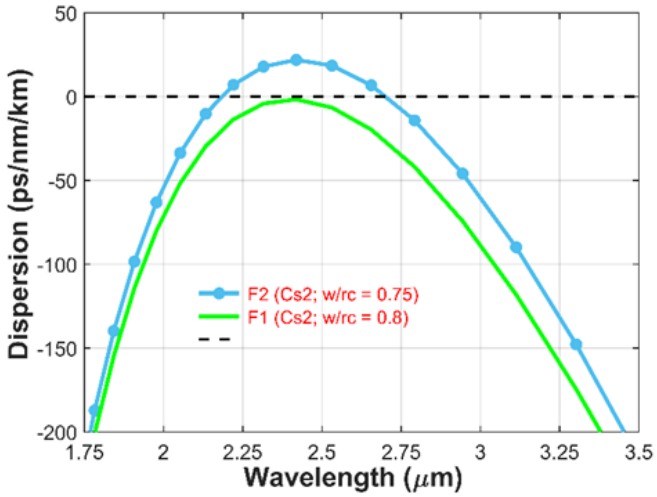

Figure 4. The dispersion properties of the proposed PCFs.

The first fiber, labeled #F1 with $w/r_c = 0.8$, exhibits an all-normal, flat, and near-zero dispersion profile, making it a promising candidate for generating SC with a broad spectrum, uniform intensity, and high coherence. The pump wavelength is set at 2.4 μm, which is close to the maximum of its dispersion curve. In contrast, the second fiber, #F2 with $w/r_c = 0.75$, demonstrates a flat anomalous dispersion regime, allowing for the generation of a broader SC spectrum compared to the all-normal dispersion case. For this fiber, the pump wavelength of 2.3 μm is chosen, which lies above its ZDW. The dispersion values at the pump wavelength for fibers #F1 and #F2 are −1.63 ps/nm/km and 7.34 ps/nm/km, respectively. The loss, effective mode area, and nonlinear coefficient of fiber #F1 at the pump wavelength of 2.4 μm are 19.16 dB/m, 1.16 μm^2, and 51.88 ($W^{-1}.km^{-1}$), respectively. In contrast, for fiber #F2 at the pump wavelength of 2.3 μm, the corresponding values are 9.64 dB/m, 1.12 μm^2, and 56.07 ($W^{-1}.km^{-1}$), respectively.

The results from the above analysis demonstrate that it is possible to control the zero dispersion wavelength and the shape of the dispersion characteristics of SCF fibers by filling the holes with CS_2. When CS_2 is filled into the holes, the dispersion curve decreases. The dispersion curves are flatter and closer to the near-zero dispersion band. The proposed SCF fibers are good candidates for SC generation applications with a broad spectrum and low peak power.

4. Conclusion

In this study, we demonstrated that infiltrating the air holes of SCFs with CS_2 markedly alters the dispersion behavior of SCFs fabricated from As_2Se_3 glass. The resulting fibers exhibit flattened and reduced dispersion compared to conventional air-hole SCFs, with variations typically remaining below 100 ps/nm/km. Such flat dispersion is crucial for achieving efficient supercontinuum generation. Additionally, the zero-dispersion wavelength was found to shift toward longer wavelengths. This adjustment of dispersion properties, together with the alignment of the ZDW with the pump wavelength, is highly desirable for broadband SCG. The proposed SCFs show low dispersion in both the normal and anomalous regimes, confirming their strong potential for generating supercontinuum light with broadened output spectra.

Acknowledgments

This research is funded by Vietnam National Foundation for Science and Technology Development (NAFOSTED) under grant number 103.03-2023.01.

Dang Van Trong was funded by the Master, PhD Scholarship Programme of Vingroup Innovation Foundation (VINIF), code VINIF.2024.TS.022.

References

[1] K. Gauthron, J. S. Lauret, L. Doyennette, G. Lanty, A. A. Choueiry, S. J. Zhang, A. Brehier, L. Largeau, O. Mauguin, J. Bloch, E. Deleporte, Optics Express, Vol. 18, 2010, pp. 5912–5919, https://doi.org/10.1364/OE.18.005912.

[2] Y. Cho, B. Park, J. Oh, M. Seo, K. Lee, C. Kim, T. Lee, D. H. Woo, S. Lee, H. M. Kim, H. J. Lee, K. Oh, D. I. Yeom, S. R. Dugasani, S. H. Park, J. H. Kim, Optics Express, Vol. 23, No. 10, 2015, pp. 13537-13544, https://doi.org/10.1364/OE.23.013537.

[3] J.C. Knight, J. Broeng, T. A. Birks, P. St. J. Russell, Science, Vol. 282, No. 5393, 1998, pp. 1476-1478, https://doi.org/10.1126/science.282.5393.1476.

[4] R. F. Cregan, B. J. Mangan, C. Knight, T. A. Birks, P. St. J. Russell, P. J. Roberts, D. C. Allan, Science, Vol. 285, No. 5433, 1999, pp. 1537-1579, https://doi.org/10.1126/science.285.5433.1537.

[5] T. T. Alkeskjold, PhD Thesis, Department of Communication, Optics & Materials, Technical University of Denmark, 2005.

[6] J. M. Dudley, G. Genty, S. Coen, Reviews of Modern Physics, Vol. 78, 2006, pp. 1135-1184, https://doi.org/10.1103/RevModPhys.78.1135

[7] W. Jin, J. Ju, H. L. Ho, Y. L. Hoo, A. Zhang, Frontiers of Optoelectronics, Vol. 6, 2013, pp. 3-24, https://doi.org/10.1007/s12200-012-0301-y.

[8] G. Stepniewski, R. Kasztelanic, D. Pysz, R. Stepien, M. Klimczak, R. Buczynski, Optical Materials Express, Vol. 6, No. 8, 2016, pp. 2689-2703, https://doi.org/10.1364/OME.6.002689.

[9] L. Dong, B. K. Thomas, L. Fu, Optics Express, Vol. 16, 2008, pp. 16423, https://doi.org/10.1364/OE.16.019629.

[10] A.Yu, Chamorovskiy, S. A. Nikitov, Journal of Communications Technology and Electronics, Vol. 58, 2013, pp. 879-890, https://doi.org/10.1134/S1064226913060053.

[11] B. Guo, Y. Wang, C. Peng, H. L. Zhang, G. P. Luo, H. Q. Le, C. Gmachl, D. L. Sivco, M. L. Peabody, A. Y. Cho, Optics Express, Vol. 12, No. 1, 2014, pp. 208-219, https://doi.org/10.1364/OPEX.12.000208.

[12] G. P. Agrawal, Nonlinear Fiber Optics, 4th ed., Academic Press, New York, 2007.

[13] A. Schliesser, N. Picqué, T. W. Hänsch, Nature Photonics, Vol. 6, 2012, pp. 440-449, https://doi.org/10.1038/nphoton.2012.142

[14] R. Wilson, H. Tapp, TrAC Trends in Analytical Chemistry, Vol. 18, No. 2, 1999, pp. 85-93, https://doi.org/10.1016/S0165-9936(98)00107-1.

[15] P. Domachuk, N. A. Wolchover, M. C. Golomb, A. Wang, A. K. George, C. M. B. Cordeiro, J. C. Knight, F. G. Omenetto, Optics Express, Vol. 16, 2008, pp. 7161-7168, https://doi.org/10.1364/OE.16.007161.

[16] C. Xia et al., IEEE Journal of Selected Topics in Quantum Electronics, Vol. 15, 2009, pp. 422, https://doi.org/10.1109/JSTQE.2008.2010233

[17] R. Buczynski, H.T. Bookey, D. Pysz, R. Stepien, I. Kujawa, J. E. McCarthy, A. J. Waddie, A. K. Kar, M. R. Taghizadeh, Laser Physics Letters, Vol. 7, No. 9, 2010, pp. 666, https://doi.org/10.1002/lapl.201010039.

[18] H. L. Van, V. C. Long, H. T. Nguyen, A. M. Nguyen, R. Buczynski, R. Kasztelanic, Laser Physics, Vol. 28, No. 11, 2018, 115106, https://doi.org/10.1088/1555-6611/aad93a.

[19] V. T. Hoang, R. Kasztelanic, A. Filipkowski, G. Stępniewski, D. Pysz, M. Klimczak, S. Ertman, V. C. Long, T. R. Woliński, M. Trippenbach, K. D. Xuan, M. Śmietana, R. Buczyński, Optical Materials Express, Vol. 9, 2019, pp. 2264-2278, https://doi.org/10.1364/OME.9.002264.

[20] L. C. Van, V. T. Hoang, V. C. Long, K. Borzycki, K. D. Xuan, V. T. Quoc, M. Trippenbach, R. Buczyński, J. Pniewski, Laser Physics, Vol. 30, 2020, pp. 035105, https://doi.org/10.1088/1555-6611/ab6f09.

[21] T. M. Monro, W. Belardi, K. Furusawa, J. C. Baggett, N. G. R. Broderick, D. J. Richardson, Sensing with Microstructured Optical Fibres, Measurement Science and Technology, Vol. 12, No. 7, 2001, pp. 854-858, https://doi.org/10.1088/0957-0233/12/7/318.

[22] K. M. Kiang, K. Frampton, T. M. Monro, R. Moore, J. Tucknott, D. W. Hewak, D. J. Richardson, H. N. Rutt, Electronics Letters, 2002, https://doi.org/10.1049/el:20020421.

[23] V. V. R. K. Kumar, A. K. George, J. C. Knight, P. J. Russell, Optics Express, 2003, https://doi.org/10.1364/OE.11.002641.

[24] A. S. Webb, F. Poletti, D. J . Richardson, J. K. Sahu, Optical Engineering, 2007, https://doi.org/10.1117/1.2430505.

[25] O. Frazão, R. M. Silva, M. S. Ferreira, J. L. Santos, A. B. Ribeiro, Suspended-core Fibers for Sensing Applications, Photonic Sensors, Vol. 2, No. 2, 2012, pp. 118-126, https://doi.org/10.1007/s13320-012-0058-3.

[26] I. Shavrin, S. Novotny, H. Ludvigsen, Optics Express, 2013, https://doi.org/10.1364/OE.21.032141.

[27] A. Hartung, A. M. Heidt, H. Bartelt, Optics Express, 2011, https://doi.org/10.1364/OE.19.012275.

[28] X. Zou, T. Izumitani, Journal of Non-Crystalline Solids, 1993, https://doi.org/10.1016/0022-3093(93)90742-G.

[29] M. Klimczak, B. Siwicki, P. Skibinski et al., Mid-infrared Supercontinuum Generation in Soft-Glass Suspended Core Photonic Crystal Fiber, Optical and Quantum Electronics, Vol. 46, 2014, pp. 563-571, https://doi.org/10.1007/s11082-013-9802-1.

[30] U. Møller, Y. Yu, I. Kubat, C. R. Petersen, X. Gai, L. Brilland, D. Méchin, C. Caillaud, J. Troles, B. L. Davies, O. Bang, Multi-milliwatt Mid-infrared Supercontinuum Generation in A Suspended Core Chalcogenide Fiber, Optics Express, Vol. 23, No. 3, 2015, pp. 3282-3291, https://doi.org/10.1364/OE.23.003282.

[31] C. T. Le, T. H. Van, H L. Van, D. Pysz, V. C. Long, T. B. Dinh, D. T. Nguyen, Q. H. Dinh, M. Klimczak, R. Kasztelanic, J. Pniewski, R. Buczyński, K. X. Dinh, Supercontinuum Generation in All-normal Dispersion Suspended Core Fiber Infiltrated with Water, Optical Materials Express, Vol. 10, No. 7, 2020, pp. 1733-1748, https://doi.org/10.1364/OME.395936.

[32] R. Ahmad, Mid-infrared Supercontinuum Generation in Liquid-filled Chalcogenide Suspended Core Fiber, Photonics and Nanostructures - Fundamentals and Applications, Vol. 52, 2022, pp. 101080, https://doi.org/10.1016/j.photonics.2022.101080.

[33] T. N. Thi, L. C. Van, Supercontinuum Generation Based on Suspended Core Fiber Infiltrated with Butanol, Journal of Optics, Vol. 52, 2023, pp. 2296-2305, https://doi.org/10.1007/s12596-023-01323-6.

[34] K. D. Xuan, C.V. Lanh, V. C. Long, Q. H. Dinh, L. V. Xuan, M. Trippenbach, R. Buczyński, Dispersion Characteristics of a Suspended-core Optical Fiber Infiltrated with Water, Applied Optics, Vol. 56, No. 4, 2017, pp. 1012-1019, https://doi.org/10.1364/AO.56.001012.

[35] B. C. Van, M. D. Ngoc, V. C. Long, H. N. Tuan, H. L. Van, Simulation Study of Mid-infrared Supercontinuum Generation at Normal Dispersion Regime in Chalcogenide Suspended-core Fiber Infiltrated with Water, Communications in Physics, Vol. 30, No. 2, 2020, p. 151, https://doi.org/10.15625/0868-3166/30/2/14857.

[36] B. Ung, M. Skorobogatiy, Chalcogenide Microporous Fibers for Linear and Nonlinear Applications in the Mid-infrared, Optics Express, Vol. 18, 2010, pp. 8647-8659.

[37] A. I. Konyukhov, E. A. Romanova, V. S. Shiryaev, Chalcogenide Glasses as a Medium for Controlling Ultrashort IR Pulses: Part I, Optics and Spectroscopy, Vol. 110, 2011, pp. 442-448.

[38] Y. C. Li, Y. T. Kuo, P. Y. Huang, S. S. Yang, C. I. Lee, T. H. Wei, Thermal Lensing Effect of CS2 Studied with Femtosecond Laser Pulses, Physical Chemistry Chemical Physics, Vol. 17, 2015, pp. 24738-24747, https://doi.org/10.1039/C5CP01796C.

[39] H. H. Pham, D. T. Bao, Calculation of Electromagnetic Force and Temperature Distribution of Amorphous Transformers in Different Operating Modes by Finite Element Method, CTU Journal of Innovation and Sustainable Development, Vol. 16, No. 1, 2024, pp. 66-75, https://doi.org/10.22144/ctujoisd.2024.269.

[40] D. Komatitsch, R. Martin, An Unsplit Convolutional Perfectly Matched Layer Improved at Grazing Incidence for the Seismic Wave Equation, Geophysics, Vol. 72, No. 5, 2007, pp. SM155-SM167, https://doi.org/10.1190/1.2757586.

[41] S. Kedenburg, M. Vieweg, T. Gissibl, H. Giessen, Linear Refractive Index and Absorption Measurements of Nonlinear Optical Liquids in the Visible and Near-infrared Spectral Region, Optical Materials Express, Vol. 2, 2012, pp. 1588-1611, https://doi.org/10.1364/OME.2.001588.

[42] R. Cherif, A. B. Salem, M. Zghal, P. Besnard, T. Chartier, L. Brilland et al., Highly Nonlinear As2Se3-based Chalcogenide Photonic Crystal Fiber for Midinfrared Supercontinuum Generation, Optical Engineering, Vol. 49, No. 9, 2010, pp. 095002.

[43] G. P. Agrawal, Nonlinear Fiber Optics, 4th ed., Academic Press, New York, 2007.